HEEGAARD SPLITTINGS OF GRAPH MANIFOLDS.

ENRIQUE ARTAL BARTOLO, SIMÓN ISAZA PEÑALOZA,
AND MIGUEL A. MARCO-BUZUNÁRIZ

ABSTRACT. In this paper we give a method to construct Heegaard splittings of oriented graph manifolds with orientable bases. A graph manifold is a closed 3-manifold admitting only Seifert-fibered pieces in its Jaco-Shalen decomposition; for technical reasons, we restrict our attention to the *fully* oriented case, i.e. both the pieces and the bases are oriented.

In this paper we deal with graph manifolds. A closed 3-manifold M is said to be a graph manifolds if its Jaco-Shalen decomposition admits only Seifert-fibered pieces. These manifolds were classified by F. Waldhausen [14, 15] and they are completely determined by a normalized weighted graph (up to a controlled family of exceptions). For technical reasons we restrict our attention to the *fully* oriented case, i.e. we assume M oriented and we also assume that the bases of the Seifert fibrations are oriented surfaces. This is only a mild restriction and this family contains the class of 3-manifolds which appear naturally in complex geometry: boundary of regular neighbourhoods of complex curves in complex surfaces, and, in particular links of normal surface complex singularities. These manifolds admit another classification in terms of plumbing graphs, see the work of W. Neumann [8].

A *Heegaard splitting* of a closed orientable 3-manifold M is a decomposition of M as a union of two handle bodies sharing a common boundary. This common boundary is a closed orientable surface Σ. The genus of the splitting is defined as the genus g of Σ. Note that, if we see Σ as the boundary of a handle body, there are g distinguished curves in it, that correspond to the boundaries of g disks such that, cutting along them, a closed ball is obtained. In a Heegaard splitting, the same surface is seen as the boundary of two different handle bodies, so there are two families of distinguished curves. These two families of curves are enough to determine the two handle bodies, and hence they also determine the manifold M and the splitting itself. An oriented closed surface of genus g, with two families of g curves is called a *Heegaard diagram*, which represents a Heegaard splitting. Every closed oriented 3-manifold admits a Heegaard splitting [4], and [11] for details. The *Heegaard genus* of such a manifold is the minimal genus of the Heegaard splittings of M.

There are a lot of works about Heegaard splittings of Seifert fibered manifolds (the *bricks* of graph manifolds), see e.g. [3, 2, 6]. In these works, *vertical* and *horizontal* splittings are defined; our approach will make use of horizontal splittings. These ideas were also transferred to the case of graph manifolds in [13], where the structure of Heegaard splittings is studied.

The contribution of this work is to provide an explicit method to construct Heegaard splittings of a graph manifold from its plumbing graph, namely, we give a closed oriented surface with two systems of cutting curves. Recall from [8] that some moves are allowed for plumbing graphs that provide the same manifold; we can use these moves to decrease the genus of the provided Heegaard splitting even though, in general, our method does not provide a minimal splitting.

Osváth and Szabó [9, 10] defined a Floer homology for 3-manifolds using Heegaard diagrams (the so-called Heegaard-Floer homology). Since then, Heegaard splittings have regained interest, specially when having combinatorial methods for its computation from a Heegaard diagram, see Sarkar and Wang in [12]. An interesting particular case is its application to the study of normal surface singularity invariants, specially those whose links are rational homology spheres, as in the series of works of Némethi *et al.* [5, 1, 7].

The paper is organized as follows. We start in §1 with an example on how to associate to a graph manifold a Heegaard splitting. No proof is given at this time, but the main steps of the construction are illustrated. In §2, we recall the construction of a graph manifold from its plumbing graph for further use. In §3, the main topological constructions which are needed for the Heegaard splittings are given, specially the concept of *float gluings*. The case of $\mathbb{S}^1$-fiber bundles with Euler number ± 1 is the next goal: in §4 the splitting is constructed while in §5 the Heegaard diagram is described. We follow the same structure for general $\mathbb{S}^1$-fiber bundles in §6. In §7, we study the splittings of the simplest graph manifolds which are not fibered bundles, i.e., corresponding to a simplicial graph with one edge. The general case is studied in §8. This escalonated procedure allows us to split the technical difficulties. Finally, in §9 we provide explicit examples, including a genus 3 splitting of Poincaré sphere (link of the $\mathbb{E}_8$ singularity).

1. ILLUSTRATIVE EXAMPLE

The goal of this paper is to describe an explicit Heegaard splitting of a graph manifold. It is presented in the form of a method, that we will now summarize by describing a surface with two systems of curves starting from of a decorated graph. We illustrate this with a suitable example.
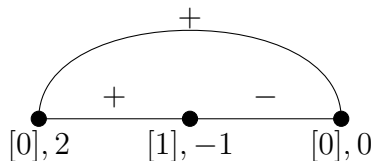
Figure 1.1. Example graph

We start with a connected decorated graph. Each vertex v is decorated with two numbers: a nonnegative integer $[g_v]$ and an integer e_v. Each edge is decorated with a sign.

From the graph, we will construct a surface, and two systems of curves inside of it (refered to as the system of *blue* curves and the system of *red* curves), following a process that mymics the construction of the graph from its elements. In this process we fix a spanning tree that determines two types of edges: edges in the tree and edges that close cycles. In our example we fix as spanning tree the straight edges. The steps to follow are the following:

(G1) For each vertex v, we consider a pair of closed oriented surfaces of genus g_v (called *top* and *bottom*) as in Figure 1.2.2 for the example.
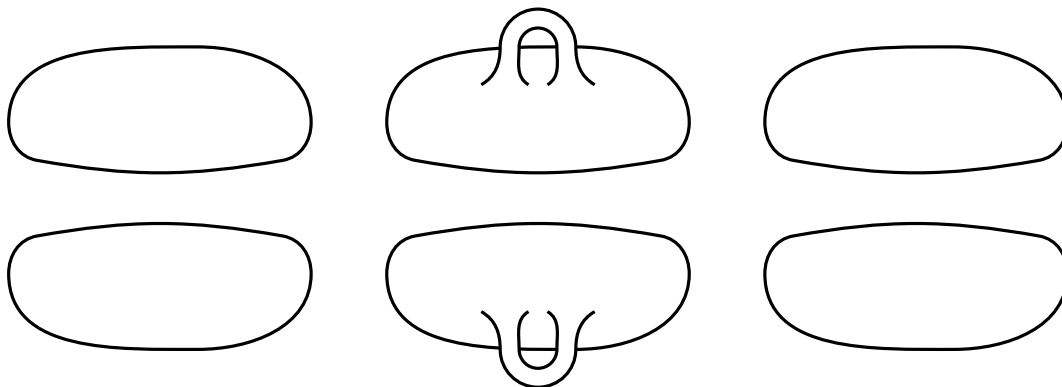

Figure 1.2

(G2) We join the surfaces of each pair by some cylinders, see Figure 1.3.3. To each one of these cylinders it will be assigned a sign, satisfying the condition that the sum of these signs in each pair of surfaces matches the number e_v. The number of these cylinders can be chosen freely, as long as the previous condition holds, and there are enough of them to perform the rest of the steps in the algorithm. Besides, one of the cylinders in each pair of surfaces is chosen as a *main cylinder* (larger in Figure 1.3.3).
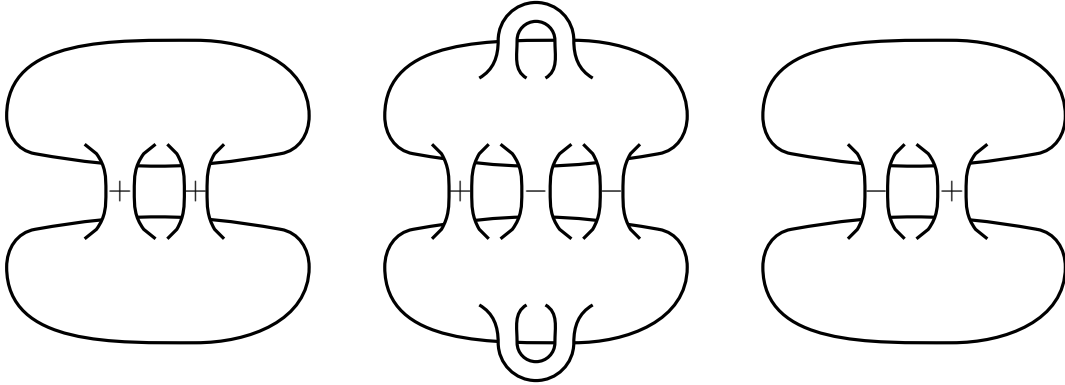
Figure 1.3

(G3) For each handle in a surface, see Figure 1.4.4, we add a red curve that turns
     around the handle meridian, passes to the other surface in the pair through
     the main cylinder, follows the same path in the other surface (reversing
     direction) and returns back to the starting point traversing again the main
     cylinder (without self intersections). Another red curve is constructed in
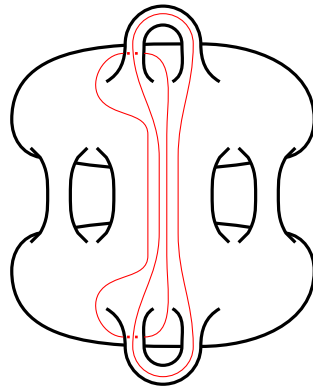   the same way but following the handle longitudes instead of the meridians.

Figure 1.4. Handle red curves of step (G3) for the surfaces of the
genus 1 vertex.

(G4) For each cylinder C which is not a main cylinder, we add a red curve that
     goes through the main cylinder and returns through C.

(G5) For each red curve, we add a blue curve. These blue curves are parallel to
     the red curves, except for performing a Dehn twist around each cylinder
     they cross. The direction of the Dehn twist is given by the sign of the
     cylinder.

(G6) Now we add the edges of the graph one by one, starting from the edges in
     the tree. To add an edge of sign s in the tree, we choose one cylinder with
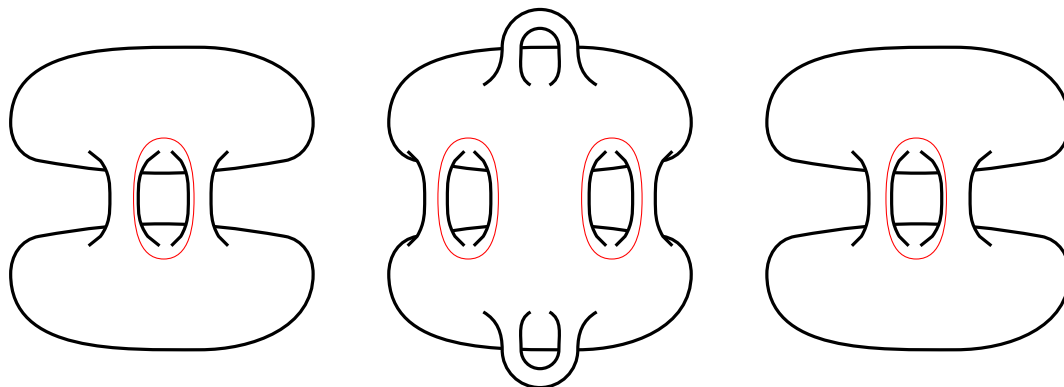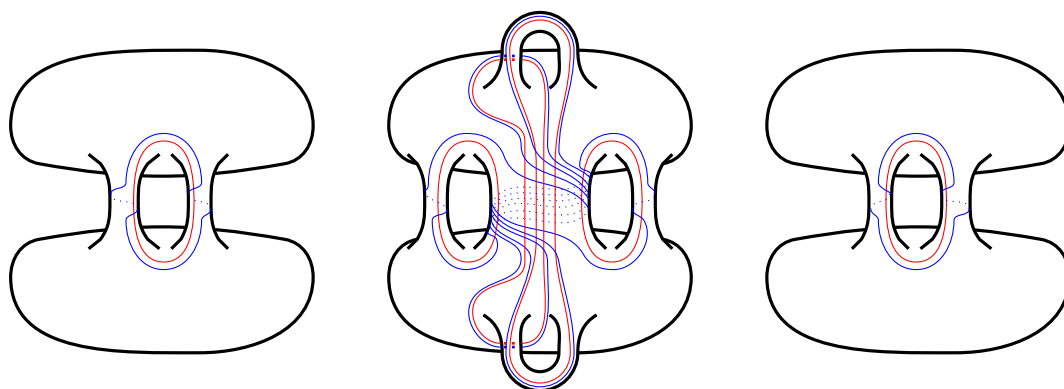
Figure 1.5. Red curves in step (G4).

Figure 1.6. All lines added after step (G5).

sign s in each of the corresponding pair of surfaces. These cylinders should be crossed only by one blue line (i.e. distinct from the main one, when the corresponding surface has either more than two cylinders or positive genus). Then we substitute these two cylinders with one cylinder that joins the upper surfaces, and another one that joins the lower ones. The red lines are just directly glued. The blue lines are also glued to form a new one. This new blue line goes parallel to the new red line in one of the new cylinders, but performs a Dehn twist around the other one. The direction of the Dehn twist will be given by the sign s of the edge.

(G7) If the edge creates a loop, we choose cylinders and substitute them by new ones as before. The two red lines δ_r and γ_r are substituted by two new ones. The first one is constructed as in (G6). In order to construct the second one we choose (arbitrarily) one of the old ones, say γ_r; it can be decomposed as $\gamma_1 \cdot \gamma_2$ where γ_2 is the the path contained in the tube which is going to disappear. We take two parallel copies of γ_1 and we connect
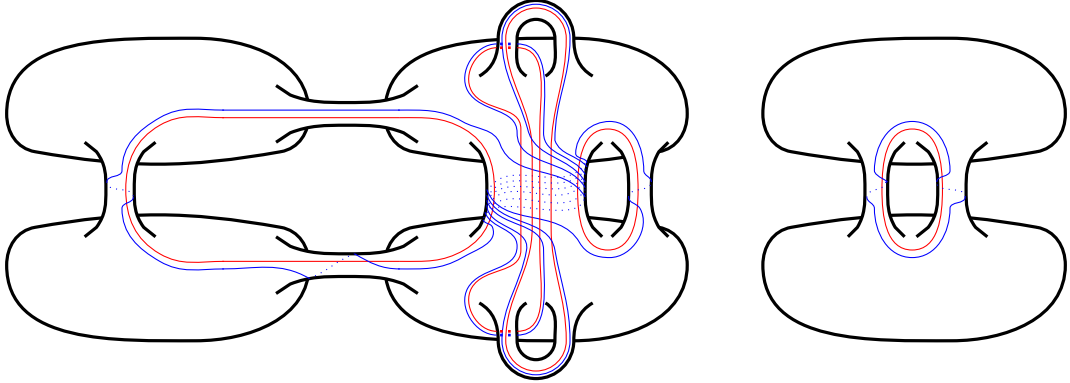
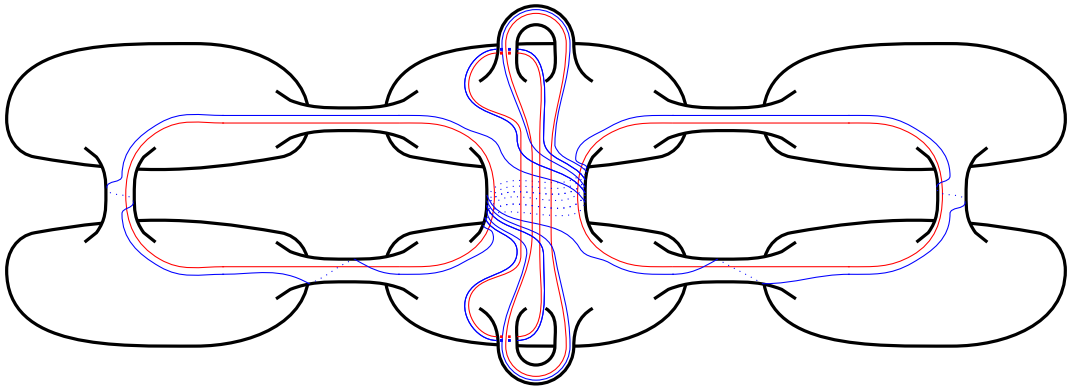Figure 1.7. Curves after adding one edge in step (G6).

Figure 1.8. Curves after adding the second edge in step (G6)

them by turning around the new cylinders in such a way that the resulting curve is disjoint with the first red curve. Let δ_b and γ_b be the two old blue lines. As before, a new blue line is obtained by gluing δ_b and γ_b as in (G6), going parallel to the corresponding red one in one of the new cylinders and performing a Dehn twist along the other one. The second new blue line is created from one of the preexisting ones (say δ_b in this example) as we did for the red one. That is, we decompose δ_b as $\delta_1 \cdot \delta_2$ where δ_2 is the the path contained in the tube which is going to disappear; we take two parallel copies of δ_1 and we connect them by turning around the new cylinders in such a way that the resulting curve is disjoint with the first blue curve.

2. PLUMBING GRAPH OF A GRAPH MANIFOLD

We recall the needed facts of Neumann's plumbing construction [8] of Waldhausen graph manifolds [14, 15]. Everything in this section is known but we recall it in order to fix notations. The *atoms* of these constructions are $\mathbb{S}^1$-fiber bundles.
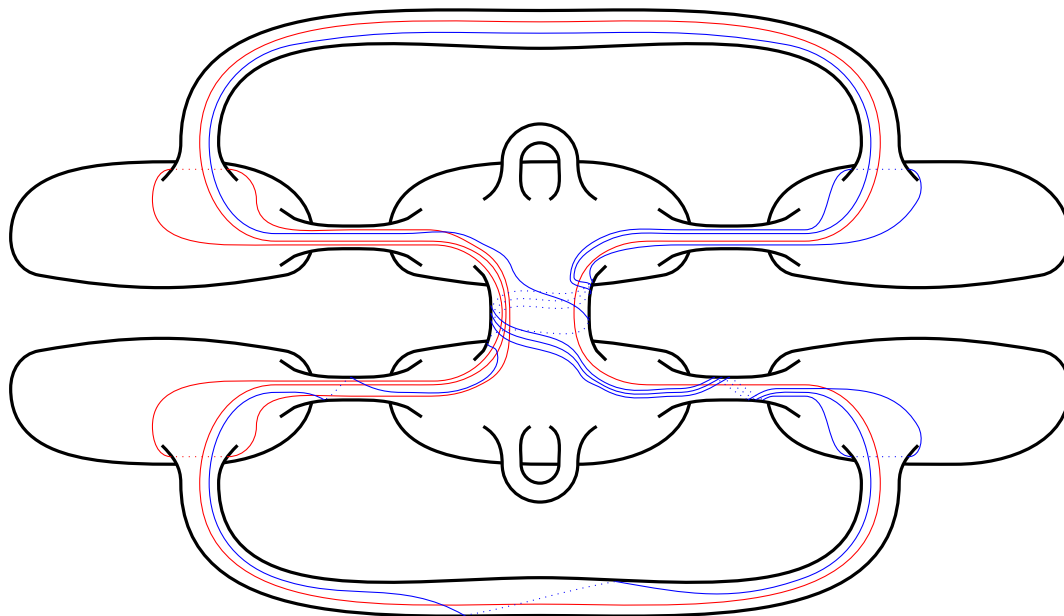
Figure 1.9. Curves after step (G7). The Handle curves have been omited for clarity.

Since the actual family we are interested in satisfies strong orientation properties we will restrict our attention to oriented graph manifolds built up using oriented fibrations.

Let $\pi : M \to S$ be an oriented $\mathbb{S}^1$-bundle over a closed oriented surface S of genus g. The oriented $\mathbb{S}^1$-bundles over a manifold N are classified by its Euler class in $H^2(N; \mathbb{Z})$. If S is an oriented closed surface there is a natural identification $\mathbb{Z} \equiv H^2(S; \mathbb{Z})$ and the Euler class is interpreted as an Euler number $e \in \mathbb{Z}$. Let us recall for further use how to compute this number. Because of the Euler class classification, any oriented $\mathbb{S}^1$-bundle over an oriented surface with boundary is homeomorphic to a product.

Let us consider a *small* closed disk $D \subseteq S$ and consider the surface with boundary $\check{S} := \overline{S \setminus D}$. The restrictions of π over D and $\check{S}$ are product bundles. Let μ_1 be the boundary of a meridian disk of the solid torus $\pi^{-1}(D)$ (oriented accordingly as ∂D) and let s_1 be the boundary of a section defined over $\check{S}$ (oriented as $\partial \check{S}$). These two simple closed curves define elements in $H_1(\pi^{-1}(\partial D); \mathbb{Z})$ as an oriented fiber ϕ_1 does. Let us use multiplicative notation for $H_1(\pi^{-1}(\partial D); \mathbb{Z})$. The fact that μ_1 and s_1 project onto opposite generators of $H_1(\partial D; \mathbb{Z})$ implies that these elements satisfy a relation

$$(2.1) \qquad\qquad s_1 \cdot \mu_1 \cdot \phi^e = 1$$

for some $e \in \mathbb{Z}$, which happens to be the Euler number of the fibration. There are several variations of this construction. The first one is very simple, we can replace $D, \check{S}$ by two surfaces S_1, S_2 with common connected boundary such that $S = S_1 \cup S_2$ and the formula (2.1) is still true. Moreover, there is no need to assume that the their boundaries are connected. Assume that $\partial S_1 = \partial S_2 = S_1 \cap S_2$ has r connected components $C_1, \ldots, C_r$; let us fix sections $s_i : S_i \to M$, $i = 1, 2$, and let us denote by s_i^j the boundary of such section in C_j (oriented as ∂S_i). Then in $H_1(C_j; \mathbb{Z})$ we have inequalities

$$(2.2) \qquad\qquad s_1^j \cdot s_2^j \cdot \phi^{e_j} = 1, \quad e_j \in \mathbb{Z},$$

and $e = e_1 + \cdots + e_r$.

Moreover, any decomposition of e as above, can be realized in this way for a given oriented $\mathbb{S}^1$-bundle with Euler number e.

A plumbing graph (Γ, g, e, o) is given by a (connected) graph Γ (without loops), a *genus* function $g : V(\Gamma) \to \mathbb{Z}_{\geq 0}$ (where $V(\Gamma)$ is the set of vertices of Γ), an *Euler* function $e : V(\Gamma) \to \mathbb{Z}$ and an *orientation* class $o \in H^1(\Gamma; \mathbb{Z}/2)$. We usually represent this graph by decorating each vertex v with $[g(v)]$ and $e(v)$, and by decorating each edge e with a sign $\sigma_e = \pm$ representing the coefficients of a cocycle (cochain) representing o. If the decoration $[g(v)]$ is not written it means that $g(v) = 0$, and empty decoration of an edge e means $+$-decoration.

Remark 2.1. If we change a cocycle by reversing the signs of all the edges adjacent to a fixed vertex, we obtain another representative of o; moreover, we can pass from one representative to another by a sequence of these moves. Of course, if Γ is a tree the o-decoration can be chosen as void.

The plumbing manifold associated to (Γ, g, e, o) is constructed as follows. First, we collect for each $v \in V(\Gamma)$ an oriented $\mathbb{S}^1$-bundle $\pi_v : M_v \to S_v$ with Euler number $e(v)$ and such that S_v is a closed oriented surface of genus $g(v)$. For each edge η with end points v, w we collect two closed disks $D_v^\eta \subset S_v$ and $D_w^\eta \subset S_w$. We choose these disks such that they are pairwise disjoint for any fixed v. Let us define $\check{M}_v$ to be the closure of $M_v \setminus \bigcup_{v \in \eta} \pi_v^{-1}(D_v^\eta)$, which is an oriented manifold whose boundary is composed by tori, as many as the valency of v in Γ. We define then $T_v^\eta := \pi_v^{-1}(\partial D_v^\eta)$. In each one of these tori we have a pair of curves $(\phi_v^\eta, \mu_v^\eta)$, where μ_v^η is a meridian of the solid torus $\pi_v^{-1}(D_v^\eta)$ (oriented as ∂D_v^η) and ϕ_v^η is an oriented fiber. Note that these curves induce a basis of $H_1(T_v^\eta; \mathbb{Z})$ which represents the orientation of T_v^η as part of the boundary of $\check{M}_v$.

Let us consider a homeomorphism $\Phi_{v,w}^\eta : T_v^\eta \to T_w^\eta$ such that $\Phi_{v,w}^\eta(\phi_v^\eta) = (\mu_w^\eta)^{\sigma_\eta}$ and $\Phi_{v,w}^\eta(\mu_v^\eta) = (\phi_w^\eta)^{\sigma_\eta}$. Basically, we are exchanging sections and fibers (twisted

by the sign). This map is determined up to isotopy by the matrix $\sigma_\eta \left(\begin{smallmatrix} 0 & 1 \\ 1 & 0 \end{smallmatrix} \right)$ of determinant -1. These maps are well-defined only up to isotopy and we can choose representatives such that $\Phi^\eta_{w,v} = (\Phi^\eta_{v,w})^{-1}$. Then the plumbing manifold associated to (Γ, g, e, o) is defined as:

$$\left(\coprod_{v \in V(\Gamma)} \check{M}_v \right) \Big/ \{\Phi^\eta_{v,w}\}_\eta$$

We will drop any reference to o if it is trivial.

Remark 2.2. Note that the above construction depends on a fixed choice of a cocycle. Let us fix a vertex v and consider the cocycle $\tilde{\sigma}$ given by

$$\tilde{\sigma}_\eta = \begin{cases} \sigma_\eta & \text{if } v \notin \eta \\ -\sigma_\eta & \text{if } v \in \eta \end{cases}$$

For the construction associated to $\tilde{\sigma}$ we keep the fibrations for $w \neq v$ and we consider the fibration $\tilde{\pi}_v : M_v \to (-S_v)$ which is the opposite fibration to π_v but the orientation of M_v remains unchanged. As a consequence $\tilde{\phi}^\eta_v = (\phi^\eta_v)^{-1}$ and $\tilde{\mu}^\eta_v = (\mu^\eta_v)^{-1}$, when $v \in \eta$. Note that $\tilde{\Phi}^\eta_{v,w} = \Phi^\eta_{v,w}$ and the resulting manifold is the same as above. Hence, by Remark 2.1, the manifold depends only on o and not on the particular choice of a representative cocycle.

Example 2.3. Let X be a complex surface and let $D = \bigcup_{j=1}^r D_j$ be a normal crossing compact divisor in X. Let Γ be the dual graph of D and define the functions g, e as the genus and self-intersection. Then the boundary of a regular neighbourhood of D is homeomorphic to the graph manifold of (Γ, g, e). If the intersection matrix of D is negative definite then D can be obtained as the exceptional divisor of a resolution of an isolated surface singularity. That is, the link of an isolated surface singularity is always a plumbing manifold, whose graph is the dual graph of the resolution. This example is the main motivation for this work.

The rest of the paper is devoted to proof that the construction of §1 provides a Heegaard splitting of the corresponding graph manifold described in this section.

3. Topological constructions

In this section we introduce different constructions which will be used in the sequel.

3.1. Drilled bodies.

Definition 3.1. A (g, n)-*drilled body* is a product $H_{g,n} := \Sigma_{g,n} \times I$, where $I := [0, 1]$ and $\Sigma_{g,n}$ is an oriented compact surface of genus g and n boundary components, with $n > 0$.
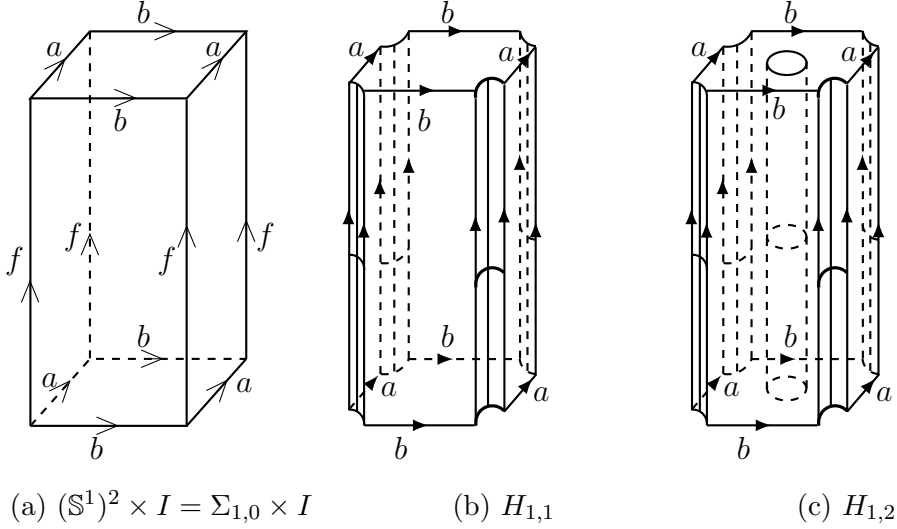

(a) $(\mathbb{S}^1)^2 \times I = \Sigma_{1,0} \times I$ (b) $H_{1,1}$ (c) $H_{1,2}$

Figure 3.1. Products

Lemma 3.2. *The boundary of a (g, n)-drilled body is an oriented surface of genus $2g + n - 1$ which is decomposed as a union of two copies of $\Sigma_{g,n}$ and n cylinders, called the* drill holes.

Proof. It is clear that $\partial H_{g,n}$ is an oriented surface for being the boundary of an oriented 3-manifold. It can be decomposed as follows:

$$\partial H_{g,n} = \Sigma_{g,n} \times \{0, 1\} \cup (\partial \Sigma_{g,n} \times I).$$

Since $n > 0$, the surface is connected. Its Euler characteristic is:

$$\chi(\partial H_{g,n}) = 2\chi(\Sigma_{g,n}) = 2(2 - 2g - n) = 2 - 2(2g + n - 1). \qquad \square$$

Theorem 3.3. *A (g, n)-drilled body is a $(2g + n - 1)$-handle body.*

Proof. We consider $\Sigma_{g,n}$ as the closure of the complement of n pairwise disjoint disks in a closed surface Σ_g of genus g. This surface is represented as a $4g$-polygon P_{4g} with the usual identifications; recall all the vertices are identified as a point P. The first disk to be removed can be chosen with center at P. The other $n - 1$ disks are in the interior of P_{4g}.

Hence the surface $\Sigma_{g,n}$ can be seen as an $8g$-gone Q_{8g}^{n-1} (with $n-1$ removed disks $D_2, \ldots, D_n$ in its interior), with identifications in $4g$ of its edges. Recall that ∂D_1 is obtained by gluing the non-identified edges of Q_{8g}^{n-1}.

We can choose $n-1$ disjoint (topological) segments α_j joining ∂D_j and ∂D_1, $j = 2, \ldots, n$. Note that if we cut along these segments and the identified edges, we obtain a topological disk.

The 3-manifold $H_{g,n}$ can be seen as a drilled prism with basis Q_{8g}^{n-1}, where the vertical faces are identified as the corresponding edges on Q_{8g}^{n-1}.

Let us cut $Q_{8g}^{n-1} \times I$ along the $2g$ identified faces and the $n-1$ topological disks $\alpha_j \times I$. We obtain the product of a disk and an interval which is a topological 3-ball. $\qquad\square$

3.2. **Float gluings.**

We are going to define another construction. Let M be an oriented 3-manifold with boundary and let η be an oriented simple closed curve in ∂M; then a regular neighbourhood C in ∂M of η is an annulus. Consider an oriented solid torus V with oriented core γ and let $\tilde{\gamma}$ be a longitude in ∂V. Let A be tubular neighbourhood of $\tilde{\gamma}$ in ∂V; note that A is an annulus. Let $\psi : C \to A$ be an orientation-reversing homeomorphism.

Proposition 3.4. *The manifold $M \cup_\psi V$ is homeomorphic to M.*

Proof. The solid torus V can be retracted to A and this rectraction induces an isotopy between $M \cup_\psi V$ and M. $\qquad\square$

Remark 3.5. Note that in the previous construction there are two possible choices for the gluing morphism ψ. One of them identifies γ with η and the other one, γ with η^{-1}. Moreover, the gluings of the boundary components of C and A are interchanged.

Definition 3.6. The above operation is called a *float gluing* of M along C.

Definition 3.7. Given a handle-body M of genus g we say that a simple closed curve $\gamma \subset \partial M$ is a *float curve* if there is a cutting system of curves in ∂M such that γ intersects this system in only one point, and this intersection is transverse.

Example 3.8. Let us consider a solid torus V_1 and let γ be a simple closed curve in ∂V_1 isotopic to the core of V_1. Let V_{g-1} be a handle-body of genus $g - 1$. Let V_g be the handle-body obtained by gluing two disks in the boundaries of V_1 and V_{g-1}; for further use, we will refer to this operation as the *handle sum* of V_1 and V_{g-1}; we can assume that γ is disjoint with the disk in ∂V_1 used for the handle sum. Then $\gamma \subset V_g$ is a *float curve* of V_g since it cuts only the meridian of V_1.

Definition 3.9. The pair (V_g, γ) is called a *standard float-curve system* of genus g.

Lemma 3.10. *Let M be a handle-body of genus g and let $\gamma \subset M$ be a float curve. Then, the pair (M, γ) is homeomorphic to a standard float-curve system of genus g.*

Proof. A handle-body can be seen as a closed ball $\mathbb{B}^3$ with $2g$ pairwise disjoint disks in the boundary glued in pairs. In this model a curve γ is a segment joining a pair of glued disks and avoiding the other ones. Two such models can be connected by a homeomorphism. $\qquad\square$

Proposition 3.11. *Let M_1, M_2 be two handle-bodies of genus $g_1, g_2 \geq 1$. Fix float curves γ_1, γ_2 in each one and consider regular neighbourhoods A_1, A_2 of these curves in $\partial M_1, \partial M_2$, respectively. Let $\psi : A_1 \to A_2$ be an orientation-reversing homeomorphism. Then, $M_1 \cup_\psi M_2$ is a handle-body of genus $g_1 + g_2 - 1$.*

Remark 3.12. If M_2 is of genus 1 the above operation is a particular case of float gluing since we only need the curve in the solid torus to be a float curve. In fact, the above proposition remains true if we only ask γ_2 to be a float curve, but we do not use this more general fact.

Proof. Note that M_2 can be constructed as a handle sum of a solid torus V_1 and a handle body of genus $g_2 - 1$. This operation can be performed in order to have $A_2 \subset V_1$ and γ_2 homotopic to the core of V_1.

Then, the gluing of M_1 and M_2 can be performed as a float gluing followed by a handle sum. $\qquad\square$

Remark 3.13. In fact, we can be more specific with the handlebody structure of $M := M_1 \cup_\psi M_2$. Consider a system of cutting curves $\alpha_1, \ldots, \alpha_{g_1}$ for M_1 and $\beta_1, \ldots, \beta_{g_2}$ for M_2. We first assume that only α_1 (resp. β_1) intersects γ_1 (resp. γ_2), at only one point and transversally (which is possible since γ_1 and γ_2 are float curves). Let $\check{\alpha}_1$ be the piece of α_1 outside the small neighbourhood of γ_1 used for the gluing; define $\check{\beta}_1$ accordingly. We can isotopically move β_1 such that $\delta := \check{\alpha}_1 \cdot \check{\beta}_1$ is a cycle in the boundary of M. Then, $\delta, \alpha_2, \ldots, \alpha_{g_1}, \beta_2, \ldots, \beta_{g_2}$ is a cutting system for M.

Remark 3.14. This process can be generalized when α_i, $1 \leq i \leq h_1$, interesects γ_1 transversally at one point and $\alpha_i \cap \gamma_1 = \emptyset$ if $h_1 < i \leq g_1$ and a similar fact arises for the other system for some h_2. In this case we can choose suitable curves α_i', $2 \leq i \leq h_2$ (resp. β_i', $2 \leq i \leq h_1$) parallel to α_1 (resp. β_1) such that $\tilde{\beta}_i := \check{\alpha}_i' \cdot \check{\beta}_i$, $2 \leq i \leq h_2$ (resp. $\tilde{\alpha}_i := \check{\alpha}_i \cdot \check{\beta}_i'$, $2 \leq i \leq h_1$) are cycles. Then

$$(3.1) \qquad \delta, \tilde{\alpha}_2, \ldots, \tilde{\alpha}_{h_1}, \alpha_{h_1+1}, \ldots, \alpha_{g_1}, \tilde{\beta}_2, \ldots, \tilde{\beta}_{h_2}, \beta_{h_2+1}, \ldots, \beta_{g_2}$$

is a cutting system of M. We can prove it using handle-slide moves of α_i (resp. β_i), $1 < i \leq h_1$ (resp. h_2), along α_1 (resp. β_1) in order to pass to the situation of Remark 3.13; after the construction of the cutting system of M we perform *inverse* handle-slide moves along δ and we recover the system (3.1).

The same idea can be used if we identify two different annuli in a single handle body.

Proposition 3.15. *Let M be a handle body of genus $g \geq 2$. Fix a cutting system of curves and two disjoint float curves γ_1, γ_2 such that they intersect different curves of the cutting system α_1, α_2. Consider regular neighbourhoods A_1, A_2 of γ_1 and γ_2 respectively. Let $\psi : A_1 \to A_2$ be an orientation-reversing homeomorphism. Then the quotient M_ψ of M by ψ is a handle body of genus g.*

Proof. Up to homeomorphism, we may assume that the float systems are standard ones. In that case, M is a handle sum of solid tori, being γ_1 and γ_2 the longitudes of two of them. The identification then produces a float gluing bewteen these two solid tori, so we obtain again a handle sum of solid tori, but introducing a loop in the chain of handle sums. This loop introduces a new handle, that compensates the one lost by the identification. $\square$
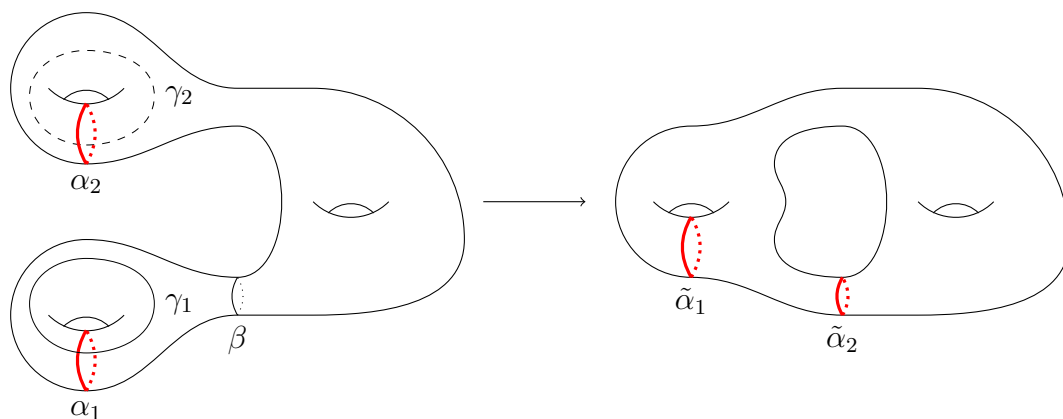

Figure 3.2. Gluing disjoint float curves in a handle body

Remark 3.16. In Figure 3.2.2 it can be seen how a new cutting curve is obtained by joining the two identified ones, and another one appears for the handle corresponding to the cycle. We are going to check that the latter corresponds to the commutator of α_1 and γ_1.

Let $F = \partial M$ and consider regular neighbourhoods $N(\gamma_1)$ and $N(\gamma_2)$ of γ_1 and γ_2 bounded by four curves $\gamma_i^{\pm}$. The surface $F_\psi := \partial M_\psi$ is obtained as follows.

Consider the quotient of $\overline{F \setminus (N(\gamma_1) \cup N(\gamma_2))}$ obtained by gluing γ_1^+ with γ_2^- and γ_1^- with γ_2^+ in order to obtain an oriented 3-manifold.

Note that $F = \partial M$ and $F_\psi = \partial M_\psi$ are equal outside regular neighbourhoods of γ_1 and γ_2. A cutting system for M_ψ can be constructed as follows. We keep the curves $\alpha_3, \ldots, \alpha_g$ of the cutting system of M and we add two new curves $\tilde{\alpha}_1$ and $\bar{\alpha}_2$. The curve $\bar{\alpha}_1$ is the connected sum $\alpha_1 \# \alpha_2$ obtained as the union of two pieces $\check{\alpha}_1, \check{\alpha}_2$ as δ in Remark 3.13. The curve $\bar{\alpha}_2$ is the image by the gluing of the curve β in M, which is the commutator of α_1 and γ_1 (see Figure 3.2.2). Note that the commutator of α_2 and γ_2 could also be chosen instead of β.

4. Heegaard splittings of $\mathbb{S}^1$-bundles over surfaces with unimodular Euler number

Let $\pi : M \to S$ be an oriented $\mathbb{S}^1$-bundle over a closed oriented surface S of genus g, with Euler number $e \in \mathbb{Z} \equiv H^2(S; \mathbb{Z})$. Consider a small closed disk $D \subseteq S$ and consider the surface with boundary $\check{S} := \overline{S \setminus D}$. Since $H^2(\check{S}; \mathbb{Z})$ is trivial, there exists a section $s_1 : \check{S} \to M$ of π. We take another *parallel* section s_2. These two sections divide $\check{M} = \pi^{-1}(\check{S})$ in two pieces M_1 and M_2; which are oriented compact 3-manifolds with boundary, and satisfy that $M_1 \cap M_2 = \partial M_1 \cap \partial M_2 = \mathbf{S} \coprod \mathbf{N}$, where $\mathbf{S} := s_1(\check{S})$ and $\mathbf{N} := s_2(\check{S})$. We will now show how to use these two pieces to construct a Heegaard splitting of M when the Euler number of the fibration is $e = \pm 1$ (i.e., the plumbing manifold associated with a graph with only one vertex v, $g_v = g$, $e_v = \pm 1$).

Convention 4.1. Once the two sections s_1, s_2 have been chosen, we choose M_1 and M_2 in such a way that the orientations on $\mathbf{N}$ induced by M_1 and s_2 coincide. This means that a positive half-fiber inside M_1 goes from $\mathbf{S}$ to $\mathbf{N}$.

The boundary of M_1 is obtained by gluing $\mathbf{S}$ and $\mathbf{N}$ with an annulus C which fibers over $\partial D = \partial \check{S}$ (whose fibers are positive half-fibers inside M_1 homeomorphic to $[0, 1]$). In the same way $\partial M_2 = \mathbf{S} \cup C' \cup \mathbf{N}$, where C' is the other annulus in M_2. Note that $C \cup C'$ is the torus $\pi^{-1}(\partial(D)) = \partial \pi^{-1}(D)$ (C and C' have common boundaries).

Proposition 4.2. *The 3-manifolds M_1, M_2 are $2g$-handle bodies.*

Proof. This manifold is, by construction, the drilled body $H_{g,1}$, see Theorem 3.3. Since M_2 is homeomorphic to M_1, it is also a $2g$-handle body. $\square$

Theorem 4.3. *Let $\tilde{M}_2 := M_2 \cup \pi^{-1}(D)$. The manifold $\tilde{M}_2$ is homeomorphic to M_2 and, hence, it is a $2g$-handle body.*

Proof. Note that C' is the annulus along which M_2 and $\pi^{-1}(D)$ are glued. Let K be the core of this annulus. Since $e = \pm 1$, K is homologous to the core of $\pi^{-1}(D)$ and the statement follows from Proposition 3.4. $\qquad\square$

Corolary 4.4. *The submanifolds M_1 and $\tilde{M}_2$ form a Heegaard splitting of M of genus $2g$.*

5. Heegaard diagram of a unimodular $\mathbb{S}^1$-bundle.

Let us denote $\Sigma_1 := \partial M_1 = \partial \tilde{M}_2$ (oriented as boundary of M_1), which is the gluing of **S**, **N** and the cylinder $C \cong \partial D \times I$. Note that **N** inherits the orientation of S while **S** inherits the opposite one.

(a) Cutting curves for M_1. (b) Cutting curves for $\tilde{M}_2$, $e = 1$.
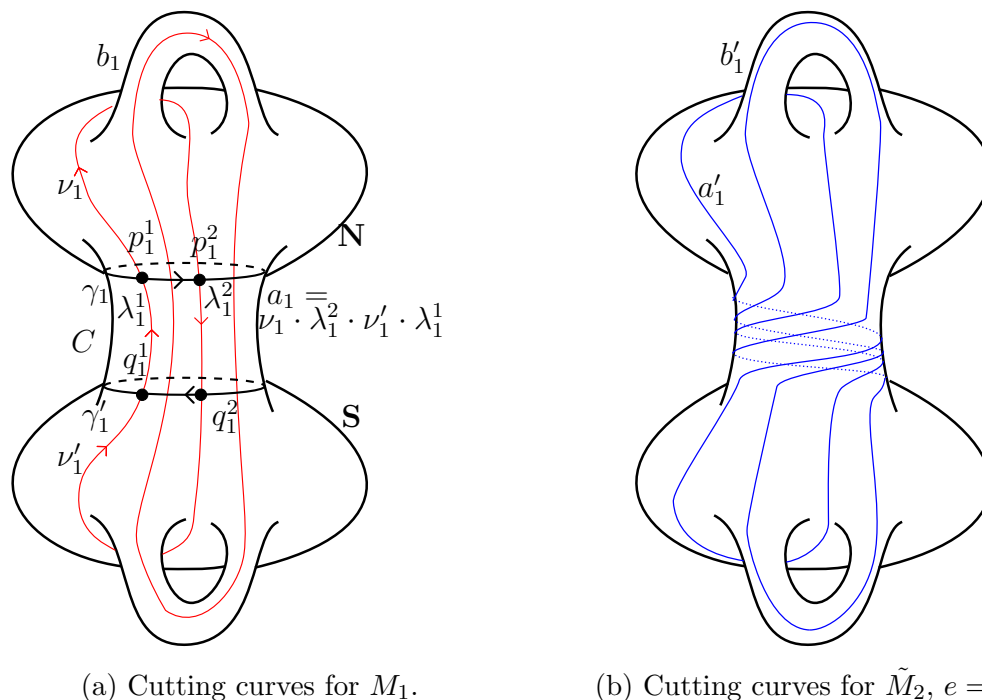
Figure 5.1

In this situation, the system of cutting curves for M_1 is formed by two families of curves:

- Curves $a_1, \ldots, a_g$ coming from half of the identified faces in the prysm, see Figure 3.1(b)alphsubfigure. They are decomposed into four pieces as follows, see Figure 5.1(a)alphsubfigure. Consider points p_i^1, p_i^2 in $C \cap \mathbf{N}$ and points q_i^1, q_i^2 in $C \cap \mathbf{S}$ such that there are half-fibers λ_i^1 (from q_i^1 to p_i^1) λ_i^2 (from p_i^2 to q_i^2). Pick up a path ν_i in **S** from p_i^1 to p_i^2 which turns around

the i'th handle like its meridian. We construct a path ν_i' in $\mathbf{N}$ in a similar way with reversed orientation. Then, $a_i := \nu_i \cdot \lambda_i^2 \cdot \nu_i' \cdot \lambda_i^1$. It is possible to choose these cycles to be pairwise disjoint.

- Curves $b_1, \ldots, b_g$ coming from the other half of the identified faces. They are constructed in the same way as the a_i, but instead of taking ν_i and ν'_i, we take paths that turn around the handles like their longitudes. These paths are chosen in such a way that they don't intersect each other and they are also disjoint to the paths a_i's.

The prysm of Figure 3.1(b)alphsubfigure shows how to prove that this is a system of cutting curves.

In order to obtain a system of cutting curves for $\tilde{M}_2$ we recall its construction. We start with M_2 (homeomorphic copy to M_1) which is constructed in the same way as M_1 but using the other cylinder C'. Recall that the union of the two cylinders C and C' along their common boundary yields the torus $\mathbb{T} := \pi^{-1}(\partial D)$, the boundary of the solid torus $\pi^{-1}(D)$. So the construction of the system of cutting curves for M_2 will mimic the one for M_1 replacing the cylinder C by C'.

Since $\tilde{M}_2 = M_2 \cup \pi^{-1}(D)$, let us consider the situation at $\pi^{-1}(D)$. In order to fix the orientations, we assume that $e = 1$, leaving the case $e = -1$ for later. The solid torus $\pi^{-1}(D)$ is represented as a cylinder whose bottom and top are glued by a vertical translation in Figure 5.2(a)alphsubfigure. Note that $\pi^{-1}(D)$ is the solid torus used in the float gluing in order to obtain $\tilde{M}_2$ from M_2.

In the torus $\mathbb{T}$, we fix the product structure with oriented section μ_1 (the boundary of a disk in the solid torus) and with oriented fibre ϕ_1. Let us fix one cutting curve (a_i or b_i) of M_1; it intersects the cylinder C in two half-fibers. Let λ_1 be the one from $\mathbf{S}$ to $\mathbf{N}$; let λ'_1 be the other half of the fiber in C' (which is part of a cutting curve in M_2) but with opposite orientation, in order to go again from $\mathbf{S}$ to $\mathbf{N}$; i.e., $\lambda_1 \cdot {\lambda'_1}^{-1}$ is homologous to ϕ_1 in $\mathbb{T}$.

The cylinders C and C' have as common boundaries two cycles $\gamma_1 \subset \mathbf{N}$ and $\gamma'_1 \subset \mathbf{S}$, oriented as boundaries of these surfaces; in Figure 5.2(a)alphsubfigure, the front part of C is coloured. The homology class of γ_1 in $\mathbb{T}$ is (with multiplicative notation) $\mu_1^{-1} \cdot \phi_1^{-e}$ (recall $e = 1$ in Figure 5.2(a)alphsubfigure), since the definition of Euler number implies that $\gamma_1 \cdot \mu_1 \cdot \phi_1^e$ is trivial.

The cycle $(\gamma'_1)^{-1} \cdot (\lambda_1 \cdot {\lambda'_1}^{-1})^e \sim \gamma_1 \cdot \phi_1^e \sim \mu_1^{-1}$ bounds a disk in $\pi^{-1}(D)$. The union of this disk with the cutting disk of M_2 containing ${\lambda'_1}^{-1}$ in its boundary provides a new disk where ${\lambda'_1}^{-1}$ is no more in its boundary. If we repeat this process with the other half-fiber in the cutting curve, we obtain the corresponding cutting curve in $\tilde{M}_2$ where the half-fibers have been replaced by curves in $C \subset \partial \tilde{M}_2 = \partial M_1$. It

can be checked that the retraction seen in Proposition 3.4 sends $\gamma_1'^{-e}\lambda_1$ to λ_1' and hence this construction provides the cutting curve for $\tilde{M}_2$.

Figure 5.1(b)alphsubfigure shows the cutting curves of $\tilde{M}_2$ for $g = 1$, $e = 1$. Note that the blue curves in C turn around as γ_1 when going from $\mathbf{S}$ to $\mathbf{N}$. The closed curve γ_1' is oriented as boundary of N and γ_1 is parallel to γ_1'.

It is clear that in the case of $e = -1$, the same thing will happen but instead of turning as γ_1, the curves will turn as γ_1^{-1}, see Figure 5.2(b)alphsubfigure.
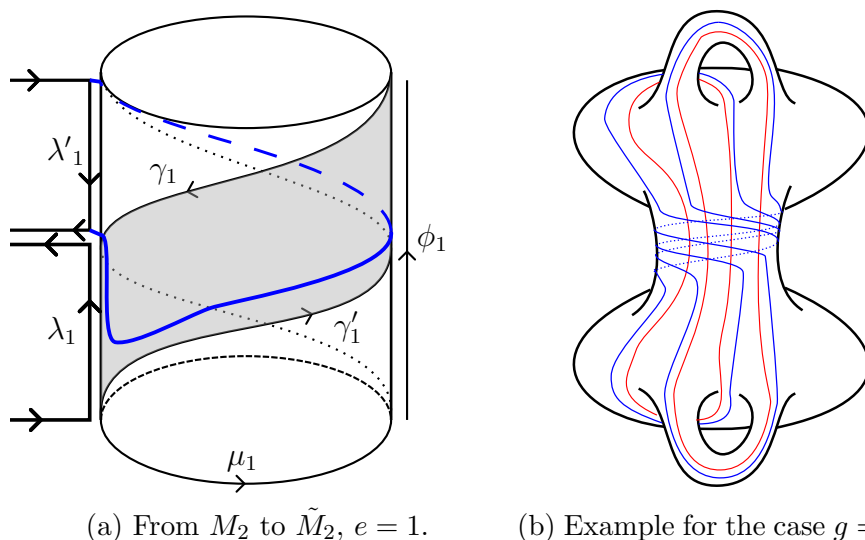
(a) From M_2 to $\tilde{M}_2$, $e = 1$.   (b) Example for the case $g = 1$, $e = -1$.

Figure 5.2

6. Heegaard splittings of arbitrary $\mathbb{S}^1$-bundles over surfaces

In order to construct a Heegaard splitting for arbitrary Euler number e we proceed as follows. Let now $\check{S} := \overline{S \setminus \bigcup_{j=1}^n D_i}$, where $D_1, \ldots, D_n$ are pairwise disjoint closed disks in S. As before, let $s_1, s_2 : \check{S} \to M$ be arbitrary parallel sections of π. For each $j = 1, \ldots, n$, let $\gamma_j := s_1(\partial D_j)$ (oriented as part of $\partial \check{S}$) and let μ_j be the boundary of a meridian disk of the solid torus $\pi^{-1}(D_j)$. By the choice of orientations the cycle $\gamma_j \cdot \mu_j \cdot \phi^{e_j}$ is trivial in $H_1(\pi^{-1}(\partial D_j); \mathbb{Z})$, for some $e_j \in \mathbb{Z}$, where ϕ is an oriented fiber of π. The following is a classical result.

Lemma 6.1. *With the above notations, $e = \sum_{j=1}^n e_j$. Moreover, for every choice of the e_j's satisfying this equality, there exists a choice of sections that realizes it.*

As we did in §4, we may decompose $\check{M} := \pi^{-1}(\check{S})$ in two pieces M_1 and M_2; M_1 and M_2 are oriented compact 3-manifolds with boundary and $M_1 \cap M_2 = \partial M_1 \cap \partial M_2 = s_1(\check{S}) \coprod s_2(\check{S})$ with the same orientation convention. From Theorem 3.3, the manifolds M_1 and M_2 are $(2g + n - 1)$-handle bodies.

Let us assume that $e_j = \pm 1$, $j = 1, \ldots, n$. Note that M_2 is homeomorphic to M_1 and hence, it is also a $(2g+n-1)$-handle body. Let $\tilde{M}_2 := M_2 \cup \bigcup_{j=1}^n \pi^{-1}(D_j)$. Following the arguments in the proof of Theorem 4.3, we can see that $M_2 \cong \tilde{M}_2$ and M_1 and $\tilde{M}_2$ have the same boundary. We have proven the following result.

Theorem 6.2. *The submanifolds M_1 and $\tilde{M}_2$ form a Heegaard splitting of M. If $e = 0$, a decomposition of this kind of genus $2g+1$ can be always obtained; and if $e \neq 0$, one of genus $2g + |e| - 1$.*

Remark 6.3. In this process, we have glued all the solid tori $\pi^{-1}(D_j)$ to M_2. This is not essential for the proof: we could have glued some of them to M_1 and the result would be equally valid.

Let us describe the cutting curves of M_1. First, we consider the cutting curves of §5. Second, we add curves c_j, $j = 2, \ldots, n$ as follows. Consider the paths α_j (as in the proof of Theorem 3.3) joining $p_j \in \partial D_1$ and $q_j \in \partial D_j$; recall that by cutting along them $\check{S}$ becomes a disk. The boundaries

$$c_j = s_1(\alpha_j) \cdot (\{q_j\} \times I) \cdot s_1(\alpha_j)^{-1} \cdot (\{p_j\} \times I)^{-1}.$$

of $\alpha_j \times I$, together with the curves of §5, form a system of cutting curves for M_1.

Following the arguments in §5, the curves of M_2 mimic the ones of M_1 except for the modification in the cylinders $\partial D_i \times I$, $1 \leq i \leq n$, due to the float gluing of the solid tori $\pi^{-1}(D_i)$. By the same reasoning as before, these modifications consist on a Dehn twist along each cylinder. The orientation of each Dehn twist depends on the sign of each e_i. Note that the cylinder $\partial D_1 \times I$ plays a special role; it will be called *main cylinder*.

Example 6.4. Figure 6.1(a)alphsubfigure shows this construction for the case of genus zero and Euler number equal to 3. We choose three solid tori and sections with $e_i = 1$. The resulting Heegaard decomposition has genus 2 and therefore is not minimal, since the manifold in question is a lens space, and as such admits a genus one decomposition. Figure 6.1(b)alphsubfigure shows an example of this construction for the case of $g = 1, e = 2$.

7. Heegaard splitting of a plumbed graph manifold with an edge

Let M be a plumbed graph manifold with an edge and two vertices. This manifold is obtained as follows. We start with two manifolds W_1 and W_2, which are oriented $\mathbb{S}^1$-bundles π_i over closed surfaces S_i of genus g_i and Euler numbers e_i, $i = 1, 2$. We take closed disks $D_{i,0} \subset S_i$ and choose a system of curves μ_i, ϕ_i on
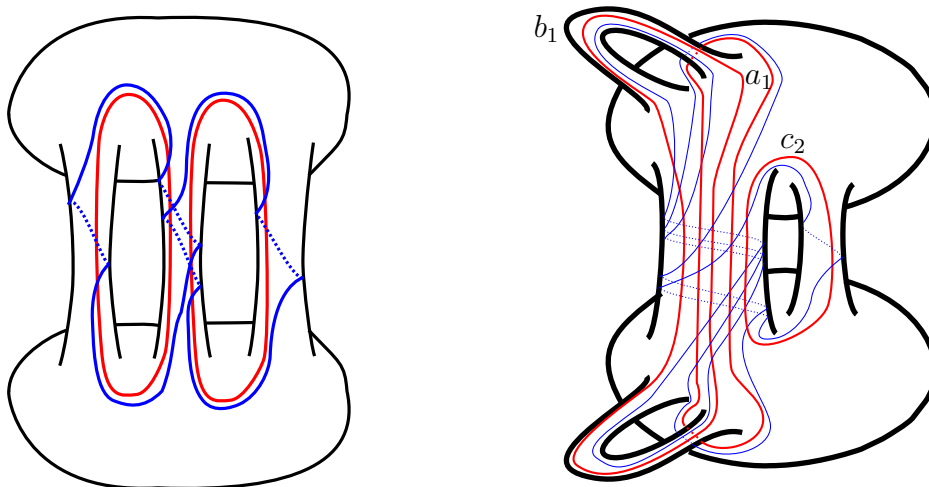
(a) Example for the case $g = 0$, $e = 3$. (b) Example for the case $g = 1$, $e = 2$.

Figure 6.1

$\pi_i^{-1}(\partial D_{i,0})$ as follows: the curve ϕ_i is an oriented fiber of π_i, and μ_i is the oriented boundary of a meridian disk of $\pi_i^{-1}(\partial D_{i,0})$.

Then, M is obtained by gluing $\pi_1^{-1}(\overline{S_1 \setminus D_{1,0}})$ and $\pi_2^{-1}(\overline{S_2 \setminus D_{2,0}})$ along their boundaries. These boundaries are tori $\pi_i^{-1}(\partial D_{i,0})$, $i = 1, 2$, and the gluing is described by a matrix in $\mathrm{GL}(2; \mathbb{Z})$ once ordered integral bases in $H_1(\pi_i^{-1}(\partial E_i); \mathbb{Z})$ are chosen. For the choice of $(\mu_{1,0}, \phi_1)$ and $(\mu_{2,0}, \phi_2)$ the matrix is $\pm \left(\begin{smallmatrix} 0 & 1 \\ 1 & 0 \end{smallmatrix} \right)$, depending on the sign of the edge as described in §2. Since the edge is contractible, the cohomology class o of §2 vanishes and can be represented by any sign, yielding to homeomorphic constructions.

Let us consider pairwise disjoint closed disks $D_{j,1}, \ldots, D_{j,n_j} \subset S_j \setminus D_{j,0}$, $j = 1, 2$. Let $\check{S}_j := \overline{S \setminus \bigcup_{i=0}^{n_j} D_{j,i}}$. We consider two parallel sections $s_{j,1}, s_{j,2} : \check{S}_j \to M_j$ of π_j as in the previous section.

As in §6, we denote $\gamma_{j,i} := s_1(\partial D_{j,i})$ (oriented as part of $\partial \check{S}_j$); let $\mu_{j,i}$ be the boundary of a meridian disk of $\pi^{-1}(D_{j,i})$. As in that section, we collect the integers $e_{j,i}$ appearing in the equalities (in homology of the boundary tori) $\gamma_{j,i} \cdot \mu_{j,i} \cdot \phi_j^{e_{j,i}} = 1$, where ϕ_j is a fiber of π_j, and they must satisfy

$$\sum_{i=0}^{n_j} e_{j,i} = e_j.$$

We impose the following conditions:

- $\min\{n_1, n_2\} \geq 2$;
- $|e_{j,i}| = 1$;

- $\varepsilon := e_{1,0} = e_{2,0}$, determining the sign of the edge.
- $\partial D_{i,0} \times I$ is not a main cylinder.

In this case, we can construct Heegaard splittings M_1^i, $\bar{M}_2^i$ of W_i as in Section 6 using the systems of disks $\{D_{j,0}, \ldots, D_{j,n_j}\}$. To do the plumbing, we have to remove $\pi_i^{-1}(\mathring{D}_{i,0})$ from $\bar{M}_2^i$, but as we saw before, this operation doesn't change the topology (since it is the inverse of a float gluing). Let's denote by $\bar{M}_2'^i$ the result of the removal of $\pi_i^{-1}(\mathring{D}_{i,0})$ from $\bar{M}_2^i$.

Note that after the plumbing, $\mu_{1,0}$ is identified with ϕ_2^ε, and $\mu_{2,0}^\varepsilon$ is identified with ϕ_1. This implies that $\gamma_{1,0}$ and $\gamma_{2,0}$ are homologous after the plumbing (because of the choice of the edge sign). In particular, it means that we can choose the sections $s_{j,i}$ in such a way that $s_{1,i}(\partial D_{1,0})$ is identified with $s_{2,i}(\partial D_{2,0})$. This way, the two Heegaard splittings are compatible, and we can extend them to a decomposition of M.

Sumarizing, we have now the following decomposition:

$$(7.1) \qquad M = \left(M_1^1 \cup M_1^2\right) \bigcup \left(\bar{M}_2'^1 \cup \bar{M}_2'^2\right).$$

Proposition 7.1. *The manifolds $M_1^1 \cup M_1^2$ and $\bar{M}_2'^1 \cup \bar{M}_2'^2$ are handle bodies, i.e., the decomposition 7.1 is a Heegaard splitting of M.*

Proof. It is enough to prove it for $M_1^1 \cup M_1^2$. We have already seen that both M_1^1 and M_1^2 are handle-bodies. We will show now that they are glued as in Proposition 3.11. In order to do so, we have to see that they are glued along annuli that are neighborhoods of a float curve.

Let us consider the torus $\pi_i^{-1}(\partial D_{1,0})$ as the product of $\mu_{1,0}$ and ϕ_1. The curves $s_{1,i}(\partial D_{1,0})$ are parallel curves that meet ϕ_1 transversally at only one point. Let

$$A_1^1 = M_1^1 \cap \pi_i^{-1}(\partial D_{1,0})$$

be the annulus along which the gluing is made. This annulus is a neighborhood of a curve parallel to $s_{1,i}(\partial D_{1,0})$.

From the construction in Section 6, we see that $\phi_1 \cap M_1^1$ is part of a cutting curve of M_1^1. And moreover, its the only intersection of a cutting curve with the torus $\pi_i^{-1}(\partial D_{1,0})$.

So the annulus A_1^1 is a regular neighborhood of a float curve in M_1^1. Analogously, A_1^2 is also a float curve in M_1^2. By Proposition 3.11, we get the result. $\qquad \square$

It is time now to describe a Heegaard diagram, i.e., to understand what happens with the cutting curves during the plumbing. Let us consider the cylinders $A_1^1 \subset M_1^1$ and $A_1^2 \subset M_1^2$ which are identified by the plumbing.

Let us fix a cutting curve λ_1 of M_1^1 which intersects once the core of A_1^1 (a float curve). In the neighborhood of A_1^1, this curve is decomposed in three connected components $\lambda_1^b, \lambda_1^c, \lambda_1^e$ where λ_1^c is the part of λ_1 that lies in A_1^1. As in §5, the path λ_1^c is a half of the fiber ϕ_1. Analogously, the cutting curve λ_2 in M_1^2 in a neighbourhood of A_1^2 can be divided in three connected components $\lambda_2^b, \lambda_2^c, \lambda_2^e$. The path λ_2^c is equivalent to a half of the fiber ϕ_2 and recall that ϕ_2 is identified with a section μ_1.

(a) Gluing of M_1^i, $e_{i,0} = 1$. (b) Gluing of $M_2'^i$, $e_{i,0} = 1$.
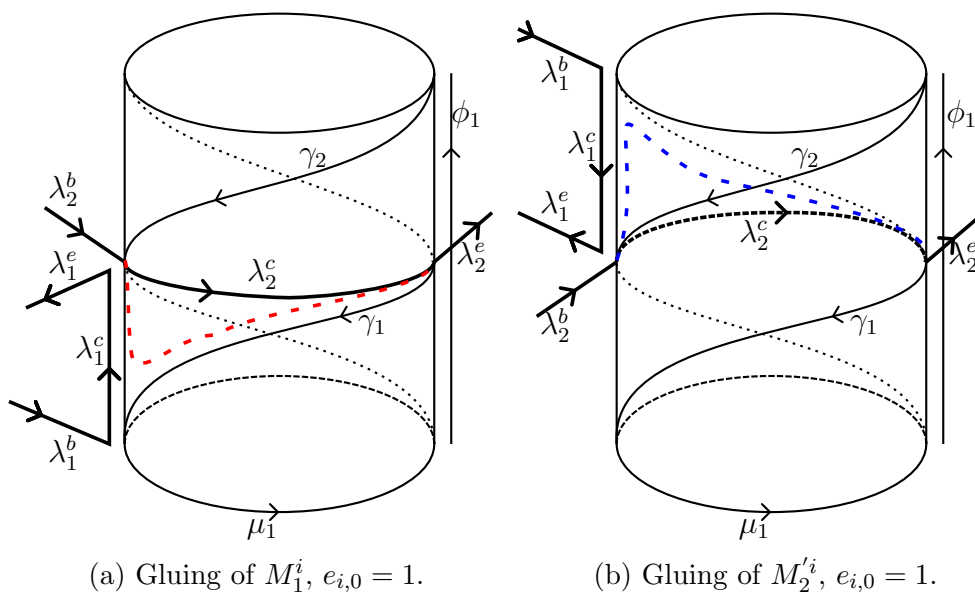
Figure 7.1

Let us decompose $\gamma_1 = \lambda_1^\gamma \cdot \lambda_1'^\gamma$ in two halves where λ_1^γ is the bottom part in Figure 7.1(a)alphsubfigure. If $e_{i,0} = 1$, we can check that λ_2^c can be isotoped inside A_1^1 to $(\lambda_1^c)^{-1}$ followed by $(\lambda_1^\gamma)^{-1}$, see Figure 7.1(a)alphsubfigure. That means that the new cutting curve $\bar{\lambda}_1$ has two connected components near $A_1^1 \equiv A_1^2$; one is $\lambda_2^b \cdot \lambda_1^e$, and the other one is $\lambda_1^b \cdot (\lambda_1^\gamma)^{-1} \cdot \lambda_2^e$.

We perform a similar argument for the gluing of $M_1'^2$ and $M_2'^2$. In this case we consider the other annuli $A_2^1 \subset M_1'^2$ and $A_2^2 \subset M_2'^2$ which become identified; they are the other parts of the plumbing tori. Let us choose cutting curves λ_1', λ_2' which go parallel near the annuli to λ_1, λ_2; in order to emphasize it, we keep the above notation for their decomposition in the neighborhood of the annuli, see Figure 7.1(b)alphsubfigure. Assuming again $e_{i,0} = 1$, we see that λ_1^c can be isotoped inside A_2^1 to λ_2^c followed by $\lambda_1'^\gamma$; note that the isotopy is done in the back part of A_2^1 if Figure 7.1(b)alphsubfigure. The new cutting curve $\bar{\lambda}_2$ has two connected components near $A_2^1 \equiv A_2^2$; one is $\lambda_2^b \cdot \lambda_1^e$, as before, and the other one is $\lambda_1^b \cdot \lambda_1'^\gamma \cdot \lambda_2^e$.

As we see in Figures 7.1(a)alphsubfigure and 7.1(b)alphsubfigure, some of the ends do not fit; in order for them to fit we have to do a half-turn around γ_1 in the suitable direction. Since we have freedom to choose the product structure in the annulus, this is equivalent to keep the intersection of the red curves as fibers, while the intersection of the blue curves perform a full loop. To be precise, since the curve $\bar{\lambda}_2 \cdot (\bar{\lambda}_1)^{-1}$ equals γ_1 near the plumbing (in homology), for $e_{i,0} = 1$ the curve λ_2 turns as γ_1 (when going from the first vertex to the second one), see Figure 7.2.2. It is easily seen that it turns as γ_1^{-1} for $e_{i,0} = -1$.
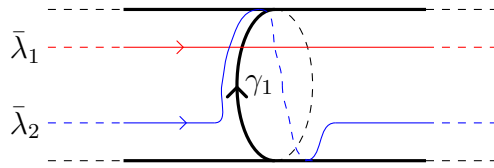
Figure 7.2. Cutting curves for $e_{i,0} = 1$.

Example 7.2. Figure 7.3.3 illustrates the case of two vertices with genus zero and both with Euler number -2. Note that we take $n_1 = n_2 = 1$ and $e_{i,j} = -1$.
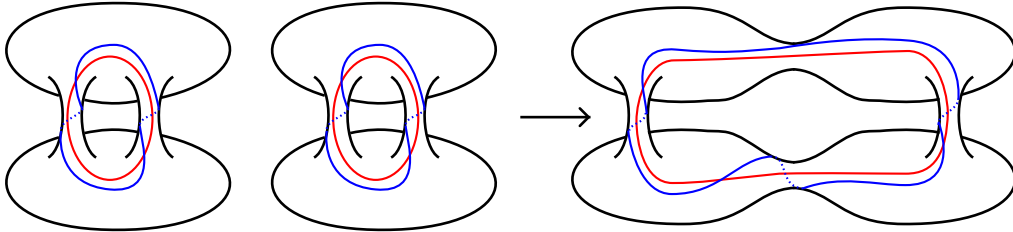
Figure 7.3. Heegaard diagram of the plumbing of two manifolds with $g = 0, e = -2$

8. Heegaard splittings of arbitrary plumbed graphs

In this section, we consider an arbitrary plumbing graph (Γ, g, e, o); for the plumbing construction we fix an explicit cocycle representing o, consisting on assigning a sign e_η to each edge η.

Fix a vertex v with valency d_v; this vertex is associated with a fibration $\pi_v : M_v \to S_v$; we choose $d_v + n_v$ pairwise disjoint closed disks in S_v, determining solid tori in M_v. The first d_v disks are assigned to a fixed edge η having v as an endpoint. As in §7, the first d_v disks will have associated numbers e_η, and

the remaining disks numbers $e_{v,j}$, $j = 1, \ldots, n_v$, such that their absolute value equals 1, and

$$\sum_{v \in \partial \eta} e_\eta + \sum_{j=1}^{n_v} e_{v,j} = e_v.$$

In general one of the extra disks will correspond to the main cylinder, hence $n_v \geq 1$. The only exception to this rule is the case $g_v = 0$, $d_v = 2$, since in this case the main cylinder plays no special role.

If Γ is a tree it is enough to iterate the construction of §7. Note also that there is no restriction for the choice of the cocyle.

Let us consider now the general case where the graph may have cycles. We start by the choice of a cocycle and a spanning tree, for which we proceed as above. Let us now explain the effect of plumbing along the remaining edges.

As we saw in Proposition 3.15, the process is different when the plumbing closes a cycle in the graph, since in that case the gluing process is done between two float curves of the same handlebody; specially, the way of constructing cutting curve systems changes. Proposition 3.15 proves that this process produces also a Heegaard splitting (where the genus remains unchanged).
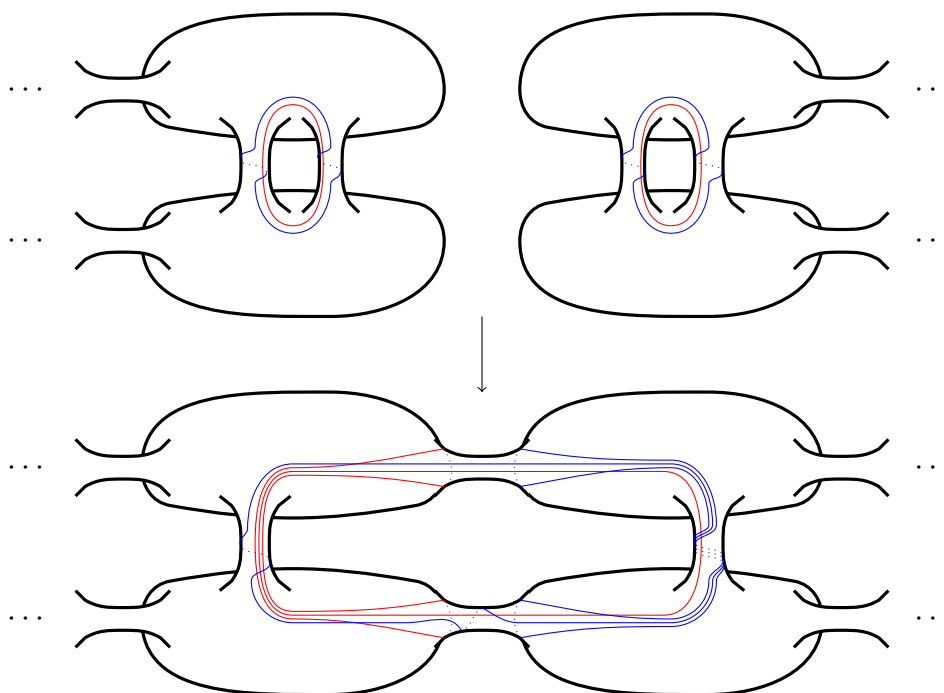

Figure 8.1. Float gluing that closes a cycle

How to obtain the cutting curves is explained in Remark 3.16. Figure 8.1.1 describes this process in our case, showing how to obtain the new pair of cutting

curves from the ones that existed before the plumbing. The first pair of cutting (red and blue) curves is obtained as in the tree case: they are obtained as connected sum of the preexistent ones. The second pair of cutting curves is constructed as explained in Remark 3.16, as the union of two parallel copies of a preexistent curve and the boundaries of the identified annuli.

9. EXPLICIT EXAMPLES

Let us consider some examples of graph manifolds for which we will give a Heegaard splitting. These examples come from links of normal surface singularities.

Example 9.1. Let M be the link of the $\mathbb{A}_n$ singularity, which is a lens space $L(n, n-1)$. The graph of this manifold is a linear tree with $n - 1$ vertices with $([0], -2)$ decorations.
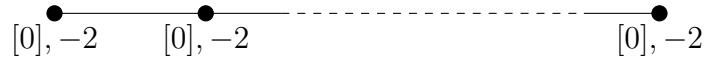
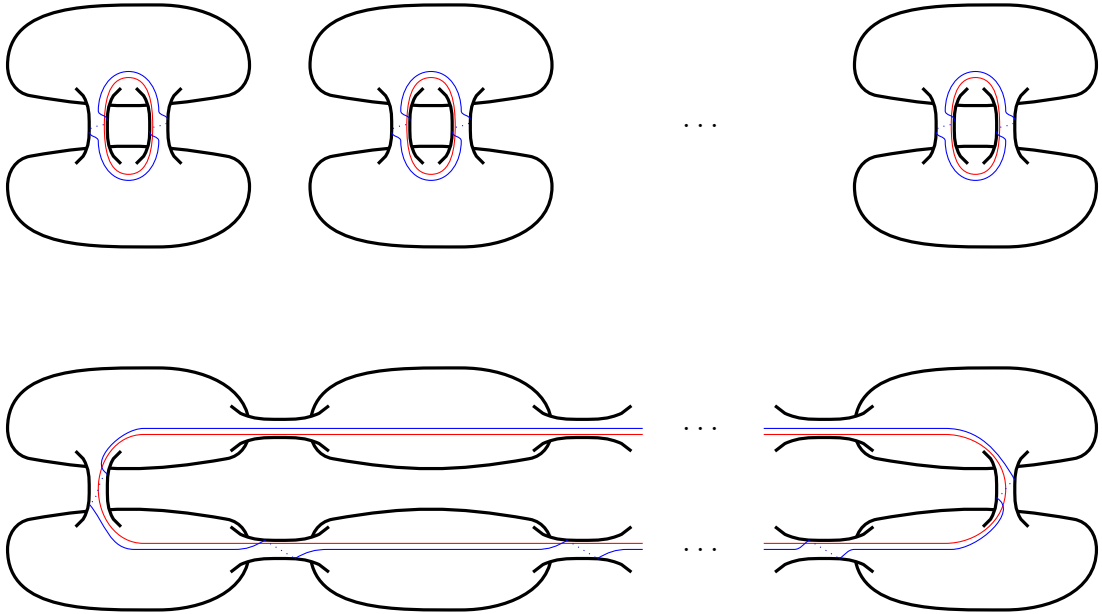Figure 9.1. $\mathbb{A}_n$ graph

Figure 9.2. Heegard diagram of the $\mathbb{A}_n$ graph.

With our method we obtain a genus 1 Heegaard splitting where the two curves intersect n times.

From now we will drop the genus weight if it vanishes.

Example 9.2. Let us consider the plumbing manifold associated with a graph with one vertex and Euler number $-n$, link of a quotient singularity, i.e. the lens space $L(n, 1)$. With our method we obtain a Heegaard splitting of genus $n - 1$. Using Neumann plumbing calculus (namely $(n-1)$ +1-blow-ups and one -1-blow-down), we can transform it in the graph of Figure 9.1.1, where the weights equal 2. The Heegaard splitting coincides with the one from the previous example, with a reversed orientation.

Example 9.3. The plumbing manifold of Figure 9.3.3 is also a lens space $L(5, 2)$ and it admits a Heegaard splitting of genus 1. However, our method provides a genus-2 Heegaard splitting.
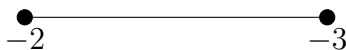

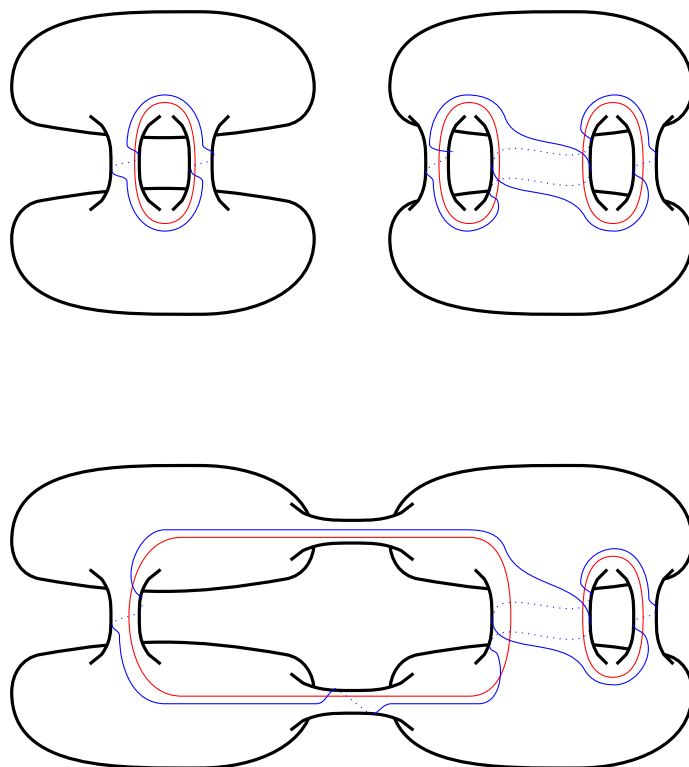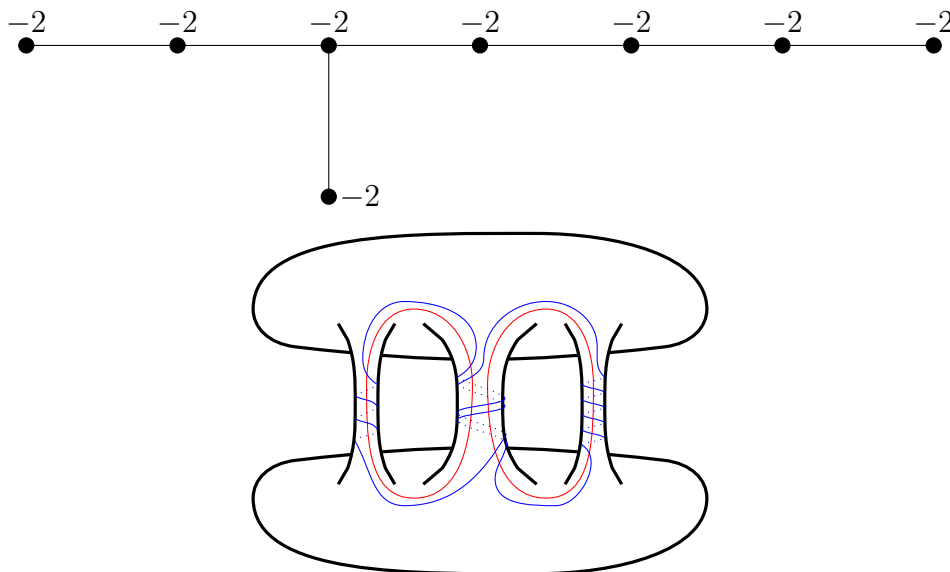Figure 9.3. A quotient singularity.

Figure 9.4. Heegaard diagram of the quotient singularity.

Example 9.4. The link of the singularity defined by $z^2 + x^3 + y^5 = 0$ ($\mathbb{E}_8$-singularity) is the Poincaré sphere. Our method provides a Heegaard splitting of genus 3, where the central vertex needs four drills (three negative ones).

Figure 9.5. Heegaard diagram of the $\mathbb{E}_8$-singularity.

It is possible to make a simpler Heegaard splitting. Using $+1$-blow-ups of [8] (and one -1-blow-down), we can modify the Euler numbers: 2 for the lower vertex and -1 in the central vertex. In that case, using the procedure in Remark 3.14, we can make a float gluing along the main cylinder, obtaining a Heegaard splitting of genus 2.

Example 9.5. The graph manifold of Figure 9.6.6 is also the link of a normal surface singularity (which cannot be quasihomogeneous) and admits a Heegaard splitting of genus 5.
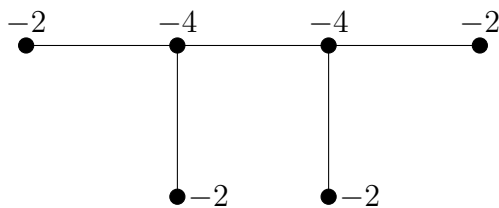

Figure 9.6. Non-Seifert manifold.

References

[1] J. Bodnár and A. Némethi, *Lattice cohomology and rational cuspidal curves*, Math. Res. Lett. **23** (2016), no. 2, 339–375. MR 3512889

[2] M. Boileau and J.-P. Otal, *Scindements de Heegaard et groupe des homéotopies des petites variétés de Seifert*, Invent. Math. **106** (1991), no. 1, 85–107.

[3] M. Boileau and H. Zieschang, *Heegaard genus of closed orientable Seifert* 3-*manifolds*, Invent. Math. **76** (1984), no. 3, 455–468.

[4] P. Heegaard, *Sur l'"Analysis situs"*, Bull. Soc. Math. France **44** (1916), 161–242.

[5] T. László and A Némethi, *Reduction theorem for lattice cohomology*, Int. Math. Res. Not. IMRN (2015), no. 11, 2938–2985. MR 3373041

[6] Y. Moriah and J. Schultens, *Irreducible Heegaard splittings of Seifert fibered spaces are either vertical or horizontal*, Topology **37** (1998), no. 5, 1089–1112.

[7] A. Némethi, *Links of rational singularities, L-spaces and LO fundamental groups*, Invent. Math. **210** (2017), no. 1, 69–83. MR 3698339

[8] W.D. Neumann, *A calculus for plumbing applied to the topology of complex surface singularities and degenerating complex curves*, Trans. Amer. Math. Soc. **268** (1981), no. 2, 299–344.

[9] P. Ozsváth and Z. Szabó, *Holomorphic disks and three-manifold invariants: properties and applications*, Ann. of Math. (2) **159** (2004), no. 3, 1159–1245.

[10] _____, *Holomorphic disks and topological invariants for closed three-manifolds*, Ann. of Math. (2) **159** (2004), no. 3, 1027–1158.

[11] D. Rolfsen, *Knots and links*, Mathematics Lecture Series, no. 7, Publish or Perish, Inc., Berkeley CA, 1970.

[12] S. Sarkar and J. Wang, *An algorithm for computing some Heegaard Floer homologies*, Ann. of Math. (2) **171** (2010), no. 2, 1213–1236.

[13] J. Schultens, *Heegaard splittings of graph manifolds*, Geom. Topol. **8** (2004), 831–876.

[14] F. Waldhausen, *Eine klasse von* 3-*dimensionalen mannigfaltigkeiten I*, Invent. Math. **3** (1967), 308–333.

[15] _____, *Eine klasse von* 3-*dimensionalen mannigfaltigkeiten II*, Invent. Math. **4** (1967), 87–117.

Departamento de Matemáticas-IUMA, Universidad de Zaragoza, Campus Plaza San Francisco s/n, E-50009 Zaragoza SPAIN

Email address: `artal@unizar.es`

Departamento de Álgebra, Universidad Complutense, Plaza de las Ciencias, n. 3, E-28040 Madrid SPAIN

Email address: `psisaza@mat.ucm.es`

Departamento de Matemáticas-IUMA, Universidad de Zaragoza, Campus Plaza San Francisco s/n, E-50009 Zaragoza SPAIN

Email address: `mmarco@unizar.es`